ELSEVIER

Thin Solid Films 308–309 (1997) 228–232

thin solid films

Production and characterisation of carbon nitride thin films produced by a graphite hollow cathode system

Stephen Muhl [a,*], Adriana Gaona-Couto [a], Juan Manuel Méndez [a], Sandra Rodil [a], Gonzalo Gonzalez [a], Alexander Merkulov [b], Rene Asomoza [b]

[a] Instituto de Investigaciones en Materiales, Universidad Nacional Autonoma de México, Apartado Postal 70-360, Coyoacan, México, D.F. 04510, Mexico
[b] Centro de Investigaciones y Estudios Avanzados, Instituto Politécnico Nacional, Apartado Postal 14-470, México D.F. 07000, Mexico

Abstract

Carbon nitride thin films have been prepared by plasma enhanced chemical vapour deposition of CH_4 and N_2 gas mixtures, by chemical transport from a hollow graphite cathode. The deposits prepared on pieces of single crystal silicon substrates were characterised using FTIR, Raman, SEM, EDX, SIMS, X-ray and electron diffraction. Single, double and triple carbon nitrogen bonds were detected in the FTIR spectra; the relative intensities of the associated bands being a function of the plasma power and substrate bias. Elemental analysis of the deposit showed that the nitrogen content was ~57 at%. A polycrystalline deposit identified as hexagonal β-C_3N_4 was obtained at low substrate temperatures. The deposit was found to grow preferentially on scratch defects on the silicon substrate surface and was stable upon annealing under vacuum up to 700°C. © 1997 Elsevier Science S.A.

Keywords: Carbon nitride thin films; Chemical vapour deposition; Plasma power; Substrate bias

1. Introduction

Carbon nitride films have become an active area of research due to the predictions of Liu and Cohen [1] of the extreme properties of β-C_3N_4, and also because of the possible applications for these materials as magnetic media coatings [2] and as semiconductors [3]. A wide variety of plasma assisted methods have been used in attempts to prepare this compound [4–8]. However, the majority of the research has resulted in deposits with nitrogen concentrations (40 at%, which is substantially less than that of the stoichiometric value ~57 at%. The purpose of this paper is to report what appears to be one of the first successes in the preparation of crystallites of C_3N_4 by a high power density physical-chemical sputtering technique assisted by ion bombardment.

2. Experimental

The reaction chamber consists of a rectangular stainless steel box, 40 × 40 × 20 cm, Fig. 1. The loadlock allows sample interchange without exposing the chamber to atmosphere. The replaceable electrode insert exposed to the plasma, internal volume ~3.5 cm^3, is made of dense nuclear grade graphite. The gases were introduced through the centre of the electrode and thereby through the graphite insert. The gas flows were controlled using MKS mass flow controllers, 100 sccm for nitrogen (99.999% purity) and 10 sccm for methane (99.999% purity), the gas pressure was measured by a MKS capacitance manometer, and this, together with a MKS variable throttle valve mounted on the mechanical vacuum pump, controlled the chamber pressure. The experiments were carried out using 1 × 1 cm pieces cut from high resistivity silicon wafers. Optimisation runs indicated that a uniform deposit could be produced with an inter electrode distance of 2 cm, gas flows of 40 and 0.75 sccm, for nitrogen and methane, with a gas pressure of 66.65 Pa. It was found that the deposition rate decreased considerably for substrate temperatures higher than 600°C. Therefore, for this study the characteristics of the deposits were determined as a function of the deposition time, the plasma power and the substrate bias. It should be noted that the plasma power density is very high; it varies from 56 to 170 Watts/cm^3. No external heating was used and

* Corresponding author.

0040-6090/97/$17.00 © 1997 Elsevier Science S.A. All rights reserved
PII S0040-6090(97)00377-5

the substrate temperature varied from 100 to 300°C dependant on the plasma power used.

The reaction chamber pre-deposit vacuum was ~2.7×10^{-4} Pa. A 13.56 MHz ENI 1 kW power supply, with a manual matching network and a Bird R.F. power meter were used to provide and measure the plasma power. The samples were analysed using a Nicolet 205 and 510P FTIR spectrophotometers (the latter has an IR microscope for small area analysis), a Dilor Micro-Raman probe using 632 nm laser light as the excitation signal, a Sloan Dektak IIA profilometer, a Siemens D500 x-ray powder diffractometer using CuKα radiation, a Leica-Cambridge Stereoscan 440 scanning electron microscope equipped with an energy dispersive x-ray analyser (EDX) for the elemental composition measurements and a JEOL JEM-1200EX transmission microscope for the electron diffraction. The samples for the electron diffraction work were prepared by slow chemical back-etching of the silicon substrates in a hydrofluoric-acetic-nitric acid solution. Etching was performed until a small hole was created in the substrate, the maskant was then removed using toluene and the sample was cleaned in iso-prolyl alcohol before analysis.

The SIMS measurements were performed using a CAMECA IMS-6F spectrometer. For the laterally resolved microprobe imaging the primary ion beam (Cs^+) had an impact energy $E_i = 5$ kV focused to a spot size of 1–2 micrometers, with a beam current $I_P = 1$ nA. The raster-scanning area was 55 μm^2 and secondary ions CsN^+ and CsC^+ were collected from the complete area. Both the EDX and SIMS elemental studies were calibrated using measurements of high purity samples of melamine ($C_3N_6H_6$) and sodium cyanide (NaCN). SIMS is a widely used technique for the characterisation of surface and thin films because of its excellent detection sensitivity. Unfortunately, the quantitative determination of major sample components is very difficult due to the extreme variation of ionisation probability of secondary ions as a function of the sample composition; the 'matrix effect' [9,10]. However, it has been observed that MCs^+ molecular secondary ions (where M is a specimen element) are fairly abundant in the sputtered flux under Cs^+ bombardment, and that for those MCs^+ species 'matrix effects' are greatly reduced [11–15]. Under steady-state conditions the flux of such species represents the bulk concentration of this element and, thus, can be measured. A number of investigations [16] have shown that under the aforementioned conditions quantification of SIMS data is possible by employing relative sensitivity factors. The reference [17] shows an example of SIMS quantification, here the NCs^+/CCs^+ intensity ratio displayed a good correlation with the C_N/C_C concentration ratio of different ternary $M_xC_yN_z$ thin film specimens. This observation was confirmed by our measurements of the two standard compounds, and the NCs^+/CCs^+ intensity ratios we obtained were 0.27 and 0.58, respectively, values that are very similar to the data presented in [17].

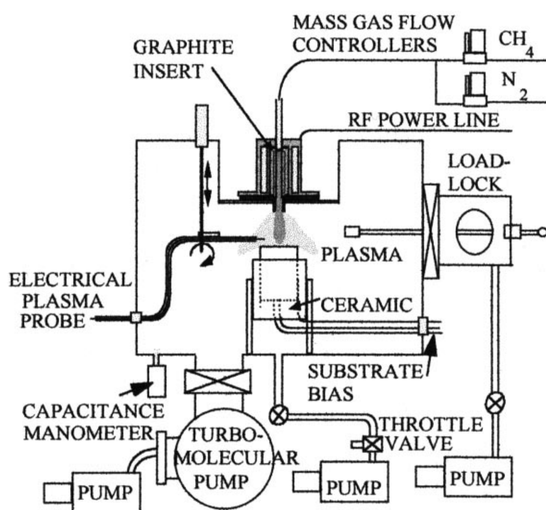

Fig. 1. Schematic drawing of the reaction chamber.

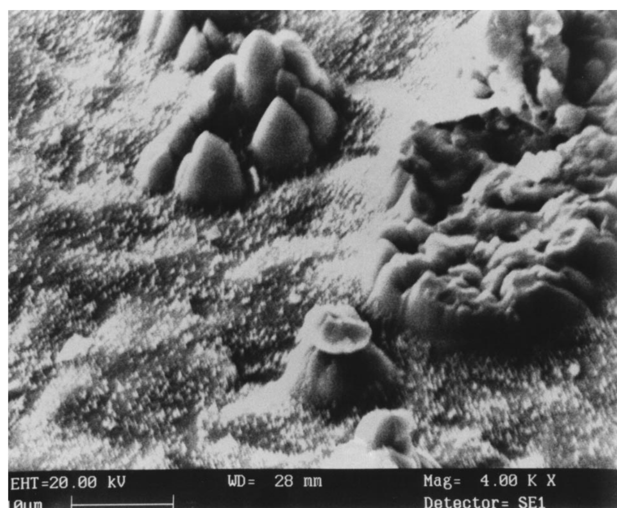

Fig. 2. Micro-photograph of the deposit surface.

Preliminary Langmuir probe measurements of the plasma involved the use of a 0.45 mm diameter tungsten wire, 6 mm long, connected to a Keithley 237 Source/Measure unit interfaced to a 486 PC.

Finally, a selection of samples were annealed for 1 h in either vacuum (1.3×10^{-4} Pa) or air, at 700 and 500°C, respectively. With the FTIR spectra of the samples being recorded before and after treatment.

3. Results and discussion

Analysis of the Langmuir probe characteristics, ~2 mm above the substrate, carried out vs. the plasma power with no substrate bias, showed that the electron temperature increased from ~3 to 15 eV for powers of 100 to 500 Watts. The corresponding change in the plasma potential was 18 to 100 Volts. The plasma density was ~10^{10} cm^{-1} for all powers. These results indicate that the plasma contains electrons with sufficient energy to cause the fragmen-

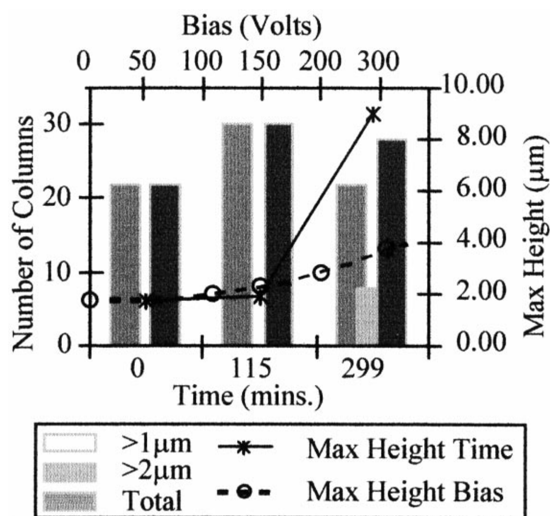

Fig. 3. Variation of the maximum column height and the distribution of the column height, for a 1-mm scan, as a function of the deposition time (bottom axis) and variation of the maximum column height vs. substrate bias (top axis).

tation of both the methane and nitrogen molecules [18,19], as well as sufficient energy to promote the formation, in the gas phase, of CN molecules [20].

During initial experiments isolated columnar growth was observed on the polished surface of the silicon substrates. The columns appeared to be associated with mechanical defects in the substrate surface. A significant increase in column growth was found for substrates that had the surface abraded with fine silicon carbide powder. Abrasion of separate areas of a substrate with various materials indicated that the existence of the columns depended on the degree of damage to the silicon and not on the inclusion of a particular material in the surface of the silicon. Given the difficulty of preparing identically abraded surfaces, the reverse matt surface of the pieces of silicon was used for the subsequent runs; reproducibility experiments indicated that this substrate gave adequate results.

Fig. 2 shows a SEM micro-photograph of a typical area of the substrate with the cone shaped columns of material, between the columns much smaller sharp peaks of deposit can be observed. The appearance of these columns is typical of a deposit formed under conditions of significant erosion due to bombardment [R. Messier, Personal Communication, MRL, Pennsylvania State University]. They were well adhered to the substrate but could be removed by mechanical scratching to obtain a powder. This powder could be used to scratch Corning 7059 glass but not sapphire plates, indicating that its hardness was within the range 9.8–18.6 GPa.

The irregular surface of the deposits signified that meaningful thickness measurements of the samples by profilometry were not possible. However this technique did give useful information about the maximum height and number of columns. These results are presented in the Fig. 3 and it can be seen that the column growth process was not linear with time. The maximum column height increased slowly as a function of the substrate bias. The variation as a function of the plasma power was more complicated, and further work is required to explain the behaviour observed. The data concerning the distribution of column heights is presented as the number of columns with heights greater than 1 micron (A), the roughness of the substrate, and those greater than 2 microns (B). The number of A columns increased vs. the deposition time until for deposition times of 300 min about half of the columns were of size B, but with a total number approximately the same as for a deposition time of 120 min. The existence of both types of columns as a function of negative substrate bias was seen to be complex, and at 100 volts only B size columns were observed.

Thus, it appears that there is an initial nucleation stage for the column growth after which they rapidly develop. This nucleation stage and the development can be seen to be affected by bombardment of the deposit by the plasma species.

The infrared spectra of samples were taken on the columns and the base zone of the deposit, with the micro-FTIR spectrometer (see Fig. 4). Apart from very small peaks due to NH and CH stretching, there is: a large band centred around 2200 cm^{-1} due to nitrile or double cumulated bonds [21], a double bond (C=C and C=N) region between 1600 and 1750 cm^{-1}, a graphitic band peaking at around 1560 cm^{-1} [22], and a broad feature spanning from 700 to 1250 cm^{-1}. Deconvolution of this last feature using Gaussian curves resulted in three main bands at 830, 1000 and 1210 cm^{-1}. The latter is identified with CN single bonds [23] and the first with a deformation mode of either a triazine ring or a deformation mode in a pyramidal structure with a nitrogen atom at its apex [24]. We are uncertain as to the identification of the 1000 cm^{-1} feature.

The IR signal obviously grows as more material is deposited, but the double bond and graphitic bands do not grow as fast, and even less so in the column areas. This suggests the existence of a more ordered structure and indeed X-ray

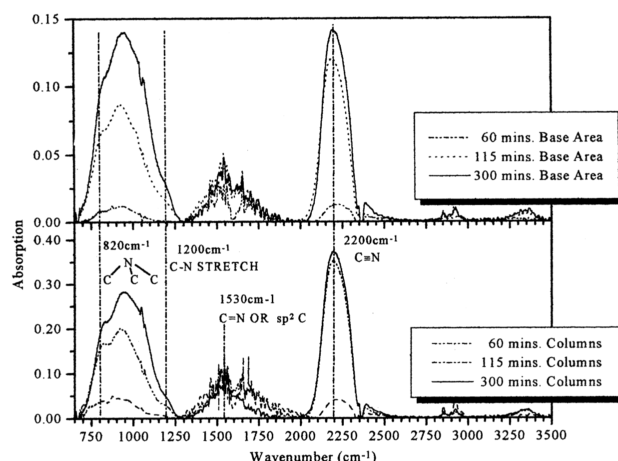

Fig. 4. Small area FTIR spectra of the column and base areas of samples prepared at different deposition times.

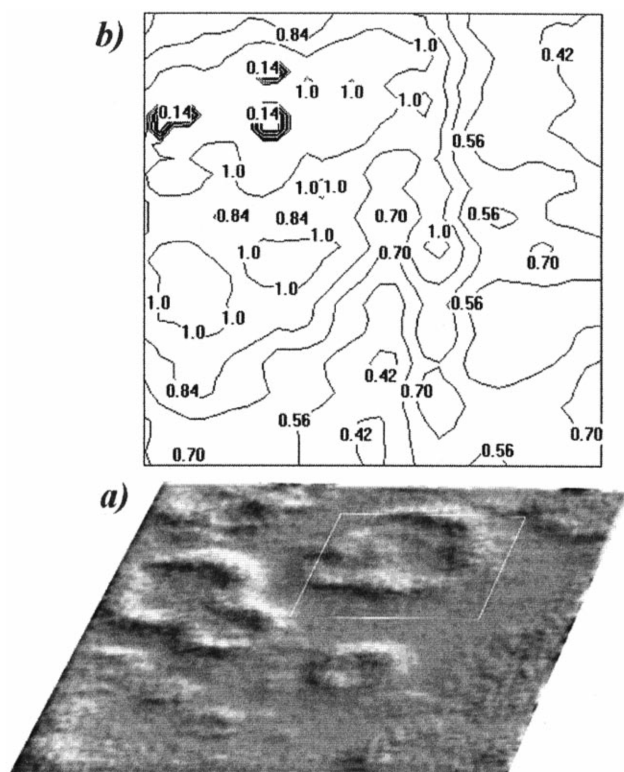

Fig. 5. Plate a is a topographical image of the deposit surface prepared using 200 W, −200 V bias and 60 min deposition time. Plate b is a C/N compositional contour map of the indicated area of plate a.

analysis of the films and electron diffraction studies indicate the presence of a crystalline phase.

Raman spectra were taken on the deposited material on both columns and non-columnar areas. For some samples the photoluminescence (PL) masked the Raman signal. A first order peak from the substrate could be seen in many of the samples, and this implies that the material is transparent to the laser light and that its bandgap should be greater than 1.96 eV. In the Raman spectra, the *G* and *D* bands of disordered graphite were detected at around 1600 and 1360 cm^{-1}, respectively, and appear in all samples indicating that there is a graphitic phase present [25]. The peaks observed in the spectrum of the sample deposited using no external bias were only observed in the columnar structures. However, we have not been able to identify these with any precise vibrational modes, except for a small feature between 600 and 700 cm^{-1} that has also been observed in CN sputtered films [26]. Such a mode has been predicted for β-C_3N_4 and has been reported by other workers [27]. There are clear differences between the Raman and the IR spectra; given that the Raman modes in graphitic CN become active in the infrared [26] it is possible to say that the infrared peaks at 830, 1000, 1200 and 2200 cm^{-1} are not from graphitic rings because they are not Raman active.

The EDX technique permitted the analysis of both the columns and the intercolumnar areas and showed that both are of the same composition, and moreover that this did not depend on the experimental variables within the ranges investigated. However, further work is required in this area as only a reduced selection of the samples with a large number of columns were analysed. After calibration measurements with the substances of known composition were performed, we found that the carbon to nitrogen ratio was 0.75 ± 0.03. This is the stoichiometric value for C_3N_4.

Fig. 5 shows result of a two dimensional SIMS analysis of a sample (200 W, −200 V bias and 60 min deposition time) using MCs^+ ions. Plate a of Fig. 5 was recorded using CCs^+ ions and supplies a topographical image of the amount of carbon in the surface studied, while plate b shows the normalised NCs^+/CCs^+ ratio from the marked part of the surface of Fig. 5a. Thus, laterally resolved ion images have been transformed into an elemental distribution map (Fig. 5b), and this shows the presence of the CN chemical phase on the sample surface.

The X-ray diffraction studies showed the presence of various fairly strong peaks at values of 2θ of 66.0, 45.2 and 43.2°, with smaller peaks at 15.8, 28.5, 41.3, 48.7, 57.5 and 69.8°. The intensity of the strong peaks were seen to increase with increasing plasma power and with the substrate bias. Indeed, the smaller peaks were only distinguishable at the highest powers and for deposition times greater than 100 min.

Electron diffraction measurement of the areas of the samples containing the (100) crystalline silicon permitted calculation of the microscope constant and this was used in the analysis of the of the sample diffraction patterns. Fig. 6 shows a typical incomplete ring diffraction pattern and bright field image from analysed the deposit. We conclude

Fig. 6. Electron diffraction pattern and bright field image of part of a column in a sample prepared using 500 W, −100 V bias and 120 min deposition time.

that the deposit consists of small crystallites (~100 nm) and since some sets of the rings were only observable when the inclination the sample was altered the crystallites are probably preferentially orientated relative to the substrate. Although the characteristic distances of the α- and β-hexagonal phases are very similar [28,29] and [Virginia Polytechnic Institute and State University, (Internet http://www.mse.vt.edu)], the α-phase has planes near to 0.15 nm and since these are not observed this phase is not present. Similarly, the β cubic phase can be excluded by the absence of distances greater than 0.22 nm, together with the existence of the 0.73 nm reflection. Similar comparisons can be carried out to rule out the presence of the pseudo-cubic and graphite phases. Therefore, it is concluded that the deposit consists of orientated crystallites of β-hexagonal C_3N_4.

The annealing studies showed no change in the FTIR spectra of the samples treated under vacuum even at 700°C, and the only alteration seen at 500°C in air was an increase in the Si-O signal probably arising from oxidation of the back surface of the substrate.

Therefore, in summation, the results show that the formation of CN compounds in the gas phase together with particle bombardment of the growing surface are important for the production of the carbon nitride deposit and that once column formation has started these grow at the expense of other areas. The FTIR and Raman spectra indicate that the deposit is a mix of CN and graphite. The EDX and SIMS reveals that the composition of the column areas is that of C_3N_4 + graphite, the contradicting results from these techniques for the base areas may be produced by the large uncertainties in the EDX measurements resulting from the small amount of material in these areas. The diffraction analysis affirmed that crystalline C_3N_4 is present in the columns and that this is the β hexagonal phase.

4. Conclusions

Deposits containing carbon and nitrogen in amounts equal to the stoichiometric value of C_3N_4 have been prepared by a high power density hollow cathode plasma assisted method which involves both chemical and physical sputtering of a graphite target by nitrogen. Plasma probe measurements showed that the electron temperature of the plasma produced with this hollow cathode reactor, in the substrate region, under near optimum conditions is remarkable high. The deposits show a columnar structure, of dimensions up to ~20 μm diameter and 15 μm high, with a hardness between 9.8–18.6 GPa. The observed cone shape of the columns is very similar to that seen in other deposits where bombardment of the coating plays a definitive role [26]. Electron and X-ray diffraction showed that the deposit has polycrystalline β hexagonal structure. The FTIR, Raman and SIMS analysis indicate that the C_3N_4 crystallites are mixed with graphite. Preliminary annealing studies show that the deposits are stable up to 700°C.

Acknowledgements

We take the opportunity to thank Jose Guzman, Ernesto Sanchez, Leticio Baños, Dr Enrique Sansores and Dr Enrique Camps for their help with the electron microscopy, small area FTIR, X-ray diffraction studies, theoretical X-ray data calculations and the plasma probe analysis, respectively. We also acknowledge the financial support of the CONACyT (projects 3333-A9308 and F278-A9208), DGAPA (IN105094) and the European Union C11*-CT93-0039 (DG12 HMSU).

References

[1] A.Y. Liu and M.L. Cohen, *Science, 245* (1989) 841.
[2] A. Krushudov, K. Kato and S. Daisuke, *J. Vac. Sci. Techol., A14* (1996) 2935.
[3] S.R.P. Silva and G.A. Amaratunga, *J.Thin Solid Films, 270* (1995) 194.
[4] M.Y. Chen, D. Li, X. Lin, V.P. Dravid, Y.-W. Chung, M.-S. Wong and W.D. Sproul, *J. Vac. Sci. Technol., A11* (1993) 521.
[5] C.M. Lieber and Z. Zhang, *J.Adv. Mater. 6* (1994) 497.
[6] L. Maya, D. Cole and E.W. Hagaman, *J. Am. Ceram. Soc., 74* (1991) 1686.
[7] R. Kalish, R. Kalis, O. Amir, R. Brener, R.A. Spits and T.E. Derry, *Appl. Phys., A52* (1991) 48.
[8] A. Hoffman, I. Gouzman and R. Brener, *Appl. Phys. Lett., 64* (1994) 845.
[9] A. Benninghoven, F.G. Rurenauer and H.W. Werner, *Secondary Ion Mass Spectroscopy*, Wiley, New York, (1987).
[10] R.G. Wilson, F.A. Stevie, Magee, *Secondary Ion Mass Spectroscopy*, Wiley, New York, (1989).
[11] M.A. Ray, J.E. Baker, C.M. Loxton and J.E. Greene, *J. Vac. Sci. Technol., A6* (1988) 44.
[12] Y. Gao, *J. Appl. Phys., 64* (1988) 3760.
[13] C.W. Magee, W.L. Harrington and E.M. Botnick, *Int. J. Mass Spectrom. Ion Proc., 103* (1990) 45.
[14] H. Gnaser, H. Oechsner and Fresenius, *Surf. Interface Anal., 17* (1991) 646.
[15] H. Gnaser, H. Oechsner and Fresenius, *J.Anal. Chem., 54* (1991) 341.
[16] A. Benninghoven, Y.Nihei, R. Shimizu and H.W. Werner (eds.), *Secondary Ion Mass Spectrometry SIMS IX*, Wiley, Chichester, 1994 p. 377.
[17] H. Gnaser, *J. Vac. Sci. Technol., A122* (1994) 452.
[18] A.N. Wright and C.A. Winkler, *Active Nitrogen*, Academic Press, New York, 1968.
[19] A. Pastel and Y. Catherine, *J. Phys., D23* (1990) 799.
[20] K.J. Clay, S.P. Speakman, and S.R.P. Silva, *J. Appl. Phys., 79* (1996) 7227.
[21] D. Li, S. Lopez, Y.W. Chung, M. Wong and W.D. Sproul, *J. Vac. Sci. Technol., A13* (1995) 1063.
[22] J. Kouvetakis, A. Bandari and M. Todd, *Chem. Mater., 6* (1994) 811.
[23] A. Bousetta, M. Lu, A. Bensaoula and A. Schultz, *Appl. Phys. Lett., 656* (1994) 696.
[24] N.B Coolthup, L.H. Daly and S.E. Wiberley, *Introduction to Infrared and Raman Spectroscopy*, Academic Press, New York, 1975, p. 240.
[25] J.H. Kaufman, S. Metin and D.D. Saperstein, *Phys. Rev., B39* (1989) 13053.
[26] J. Koskinen, J.P. Hirvonen, J. Levoska and P. Torri, *Diam. Related Mater., 5* (1996) 669.